Colloid Polym Sci (2004) 282: 761–765
DOI 10.1007/s00396-003-1016-9

SHORT COMMUNICATION

Shuhua Han
Wanguo Hou
Wenxiu Dang
Jun Xu
Jifan Hu
Dongqing Li

Synthesis of rod-like mesoporous silica with hexagonal appearance using sodium silicate as precursor

Received: 21 April 2003
Accepted: 24 September 2003

S. Han · W. Hou (✉) · W. Dang · J. Xu
Laboratory of Colloid and Interface
Chemistry of State Education Ministry,
Shandong University,
250100 Jinan, P. R. China
E-mail: shuhhan@sdu.edu.cn
Tel.: +86-531-836-5450
Fax: +86-531-856-4464

J. Hu
Department of Physics,
Shandong University,
250100 Jinan, P. R. China

D. Li
Department of Mechanical and Industrial
Engineering, University of Toronto,
Ontario, M5S 3G8, Canada

Abstract Using sodium silicate as precursor, rod-like mesoporous silica with hexagonal appearance was synthesized by controlling the pH value of a mixed micelles solution of cetyltrimethylammonium bromide (CTAB) and cetyltrimethylammonium chloride (CTAC) during hydrolysis of ethyl acetate. The resulting mesoporous silica was characterized by small angle X-ray diffraction, nitrogen gas adsorption-desorption measurement and scanning electron microscopy. Results showed that the regular rod-like shapes with hexagonal appearance were obtained at a 9:1 molar ratio of CTAB to CTAC, and that the amounts and lengths of the rod-like mesoporous silica particles decreased with decreasing CTAB to CTAC molar ratio. There existed a type IV adsorption isotherm and an H1 hysteresis loop in N_2 gas adsorption-desorption curves.

Keywords Morphology · Meso porous materials · Template · Cetyltrimethylammonium bromide · Cetyltrimethylammonium chloride

Introduction

Since 1992 the development of ordered nanoporous material called M41s has aroused the interest of scientists due to its high surface areas (~1,000 m^2/g), narrow pore size distribution and attractive mesoporosity which was found to be ordered, and tunable over the region 2.0–10.0 nm [1].

Formation of the ordered mesoporous materials was determined by the interaction between precursor and surfactant molecules. When the concentration of surfactant was above its critical micelle concentration (CMC), it aggregated, depending on the experimental conditions, forming spherical micelles, rod-like micelles, hexagonally ordered crystals, cubic crystals, lamellar phases, inverse micelles or inverse micellar liquid crystals, etc. Using ordered phases as templates, silica with ordered nanostructure could be obtained through a route of S^+I^- or $S^+X^-I^+$, where S^+ = cationic surfactant; X^- = Cl^-, Br^-; I^+ = precursor [2]. On the other hand, synthesis of mesoporous silica with various morphologies was also of great interest because some important information for porous system engineering might be obtained from these materials. Mou et al. [3, 4] showed that a "tubules-within-a-tubule" hierarchical order of mesoporous silica could be synthesized by cooperative condensation of silica and cylindrical cationic micelles; Schacht et al. [5] indicated that the ordered mesoporous silica with macroscopically hollow spherical, fibrous morphology, or thin sheet was formed using oil/water microemulsion as templates. Ozin and co-workers [6] synthesized mesoporous silica with specified shapes, such as spiral, gyroid, toroidal, disk-like, and spheroidal. Zhao et al. [7] synthesized mesoporous silica with fiber, doughnut, gyroid, discoid-like and hard sphere shapes using amphiphilic triblock copolymers as structure-directing agents.

In this paper rod-like mesoporous silica was synthesized using mixed surfactants of cetyltrimethylammonium bromide (CTAB) and cetyltrimethylammonium chloride (CTAC) as templates. Because the hydrated ionic radii of bromide and chloride were different, the electric charge density of micelles varied with the change in the molar ratio of CTAB to CTAC, the latter affecting the properties of mesoporous silica. The formation mechanism of morphology of mesoporous silica was also discussed.

Materials and methods

Reagents Crystalline sodium silicate was obtained from Shanghai Fourth Reagent Plant; it contained 21.05% (w/w) Na_2O, and the molar ratio of Na_2O to SiO_2 was 1.03. A 25% aqueous solution of CTAC was from Aldrich and solid CTAB was from the Institute of Chemical Technology of Jining. Ethyl acetate was analytical grade reagent obtained from Zhangzhou Second Reagent Plant.

Synthesis Mesoporous silica was prepared using aggregates of CTAB and CTAC as template. A typical procedure was as follows: a mixture of CTAB and CTAC [the total mole number (0.01076) of mixed surfactants was kept constant but the molar ratio was varied] was dissolved in water, and 4 g of $Na_2SiO_3{\cdot}9H_2O$ was then added, with the total volume of the mixed solution kept constant (140 ml). After sonication, a clear solution was obtained. To this solution 10 ml of ethyl acetate was added and sonicated for 45 s. After hydrolysis (5 h at 30 °C), the mixture solution was kept at 80 °C for 72 h in a heating oven. The resulting solid was recovered by filtration, then washed with distilled water and ethanol, and finally dried at room temperature. The mixed surfactants were removed by calcinations at 540 °C for 6 h.

Characterization Powder X-ray diffraction data were obtained on a D/max-rB model with a Cu target at 40 kV and 120 mA, and scanning speed was 0.2°/min. Diffraction data were recorded between 1° and 10° at an interval of 0.01°. Scanning electron microscope (SEM) experiments were performed on an H-7000 transmission electron microscope with an H-7110 SEM accessory. Nitrogen gas adsorption-desorption measurement was carried out on a Omnisorp 100 CX gas adsorption analyzer from Coulter. Every sample was degassed at 350 °C for 12 h until a pressure of 10^{-5} Pa or below was reached.

Results and discussion

Mechanism of reaction

For CTAB, the critical micelle concentration (CMC) was 0.03% (0.9~1.0 mM) [8, 9]. Above the CMC, a transition from spherical to rod-like micelles occurred, and the size of micelles increased with increasing CTAB concentration, eventually resulting in long, flexible worm-like micelles. In our system, the CTAB concentration was 5.3% (0.154 M), much larger than the CMC, and it could easily form rod-like micelles due to electrostatic shielding effect of sodium silicate as electrolyte and precursor. Due to poor solubility in water, ethyl acetate was solubilized in the palisade layer of the mixed micelles of CTAB and CTAC, and hydrolyzed under catalysis of cationic micelles:

$$CH_3COOC_2H_5 = CH_3COOH + C_2H_5OH$$

Sodium silicate was neutralized by the resulting acetic acid on the surface of the mixed micelles of CTAB and CTAC. Using the rod-like micelles as templates, the ordered nanostructure silica with special morphologies could be obtained through a route of S^+I^-, where S^+ = cationic surfactant, and I^+ = precursor [2].

Morphological aspects

Morphologies of mesoporous silica are shown in Fig. 1: without CTAC, many particles were irregular and some of them were rod-like (Fig. 1a). Addition of CTAC made the number of rod-like particles increase but irregular particles decrease. The rod-like particles had regular hexagonal appearance (Fig. 1f); their diameter was about 1 μm, and their length was above 4 μm. With the decrease of the molar ratio of CTAB to CTAC (from 9:1 to 5.5:4.5) the amounts and lengths of rod-like particles deceased (Fig. 1b, c, d e), so a templating mechanism was suggested. The molecules of CTA^+ could form micelles when the concentration of CTA^+ was above CMC, and the micelles bore positive charges; Br^- and Cl^-, as counter ions, formed electric double layers on the surface of the micelles. Because of the different hydrated ionic radii of Br^- and Cl^- (the hydrated ionic radius of Br^- was smaller than that of Cl^-), the electrostatic interaction between CTA^+ and Br^- was stronger than that of CTA^+ and Cl^-, and thus CTAB easily formed long flexible worm-like micelles, while CTAC easily formed spherical micelles. The phenomenon was proven by Fabre [10], who demonstrated, using self-diffusion and NMR techniques to probe CTAB/CTAC mixtures, that Br^- ions were preferentially adsorbed on to the surface of both spherical and rod-like micelles. Therefore, in the mixed solution of CTAB and CTAC, the length of mixed rod-like micelles became shorter and shorter with the decrease of molar ratio of CTAB to CTAC. From the above analysis, we concluded that the rod-like mesoporous silica was formed based on the templates of rod-like micelles formed by CTAB and CTAC, and that the amount and the length of rod-like mesoporous silica decreased with decreasing CTAB to CTAC molar ratio.

When a small amount of acetone (the molar ratio of acetone to CTA^+ was 2:1) was added, particles became longer as compared with Fig. 1e, with the molar ratio of CTAB to CTAC being 5.5:4.5. However, with decreasing molar ratio of acetone to CTA^+ (from 2:1 to 1:1) the length of rod-like particles became shorter, and some rod-like particles curled (Fig. 2). The reason

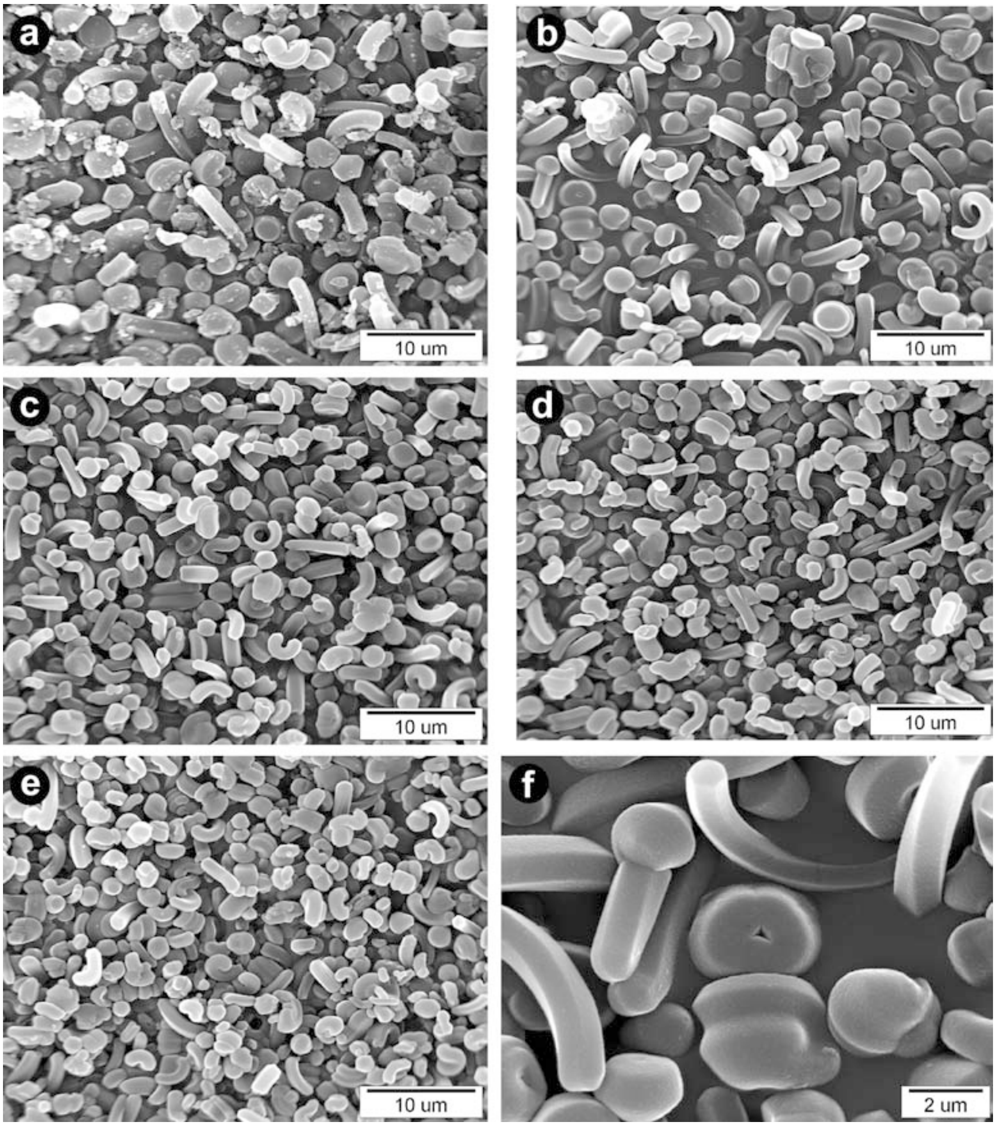

Fig. 1a–f Morphologies of mesoporous silica at varied molar ratio of cetyltrimethylammonium bromide (CTAB) to cetyltrimethylammonium chloride (CTAC). **a**10:0. **b** 9:1. **c** 8:2. **d** 6.5:3.5. **e** 5.5:4.5. **f** 9:1

acetone affected the length of rod-like particles was that acetone as cosolvent made the solubility of CTAB in water increase, the aggregation number of the micelles decrease, and the shapes of micelles change.

Phase identification from X-ray diffraction

The X-ray diffraction (XRD) patterns of mesoporous silica samples with the as-synthesis and the calcination samples at 540 °C for 6 h are shown in Fig. 3. Only one diffraction peak, indexed as (100) in the as-synthesis sample, and three diffraction peaks, indexed as (100), (110) and (200) in the calcination sample, were observed; these peaks were attributed to hexagonal symmetry [3]. The fact that there existed diffraction peaks of (110) and (200) in the calcination samples indicated that the mesoporous structure was more ordered after calcination.

The unit cell constants of mesoporous silica (according to $a_0 = 2d_{100}/3^{1/2}$) and d_{100} values are listed in Table 1. As we can see from Table 1, the d_{100} values of as-synthesis sample were larger than that of calcination sample. The reason was that calcinations resulted in shrinkage in the skeleton of the network. Also, we found that the pore-center-distance (a_0) of two adjacent pores of silica was about 4.5 nm or so, approximately twice as long as the length of carbon chain of CTA^+. This result was in agreement with that reported elsewhere [11].

N_2 gas adsorption-desorption curves of mesoporous silica

Nitrogen gas adsorption-desorption curves are shown in Fig. 4. As expected for mesoporous materials, a type IV adsorption isotherm and an H1 hysteresis loop were

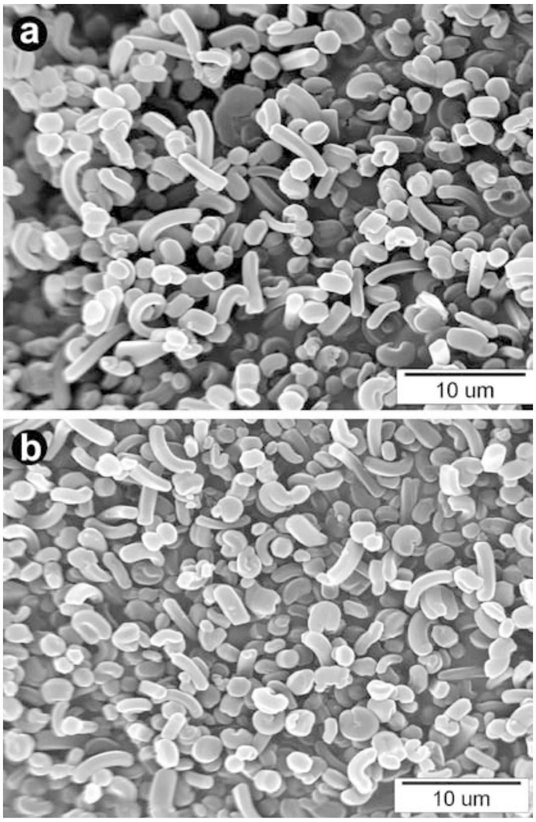

Fig. 2a, b Scanning electron microscope photographs of mesoporous silica after addition of acetone (the molar ratio of CTAB to CTAC was 5.5:4.5). **a** Acetone:CTA$^+$ = 2:1. **(b)** Acetone:CTA$^+$ = 1:1

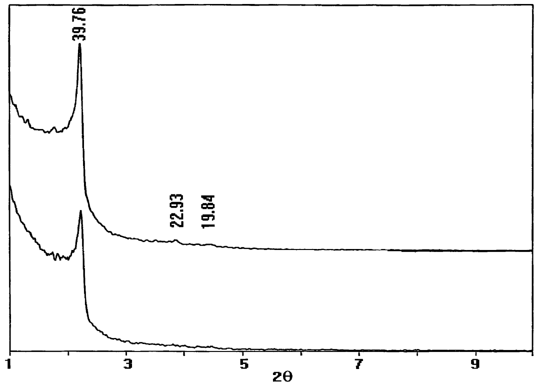

Fig. 3 X-ray diffraction patterns of mesoporous silica samples (CTAB:CTAC = 9:1) with as-synthesis and calcination at 540 °C for 6 h. *Upper curve* calcinations, *lower curve* as-synthesis

Table 1 d_{100} and a_0 of mesoporous silica at different molar ratios of CTAB to CTAC

Molar ratio of CTAB to CTAC	d_{100} (nm)		a_0 (nm)	
	As-synthesis	Calcinations	As-synthesis	Calcinations
10:0	3.99	3.96	4.61	4.57
9:1	3.98	3.98	4.59	4.59
8:2	3.98	3.94	4.59	4.55
6.5:3.5	3.96	3.92	4.57	4.53
5.5:4.5	3.96	3.94	4.57	4.55
4:6	3.96	3.94	4.57	4.55
0:10	3.94	3.91	4.55	4.51

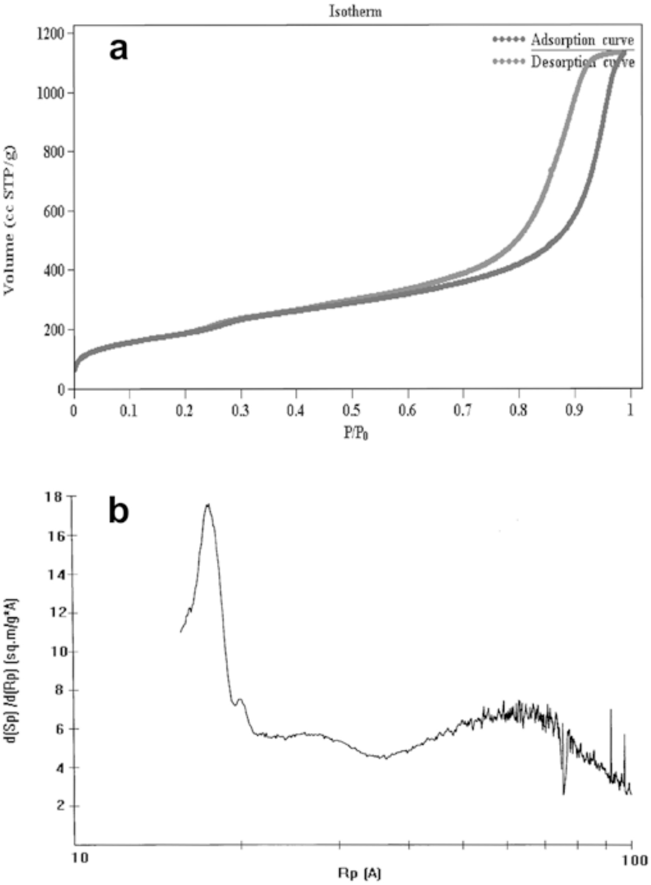

Fig. 4a, b N_2 gas adsorption-desorption and pore size distribution curves for the calcinated sample (CTAB:CTAC = 9:1). **a** N_2 gas adsorption-desorption curves. **b** Pore size distribution curves

observed [12]. In the range 0.7–1.0 Pa, step-like curves were due to capillary condensation taking place in mesoporous materials. A narrow pore-size distribution curve is observed in Fig. 4b. Brunauer-Emmett-Teller (BET) surface area, pore volume with diameter above 2 nm, thickness of pore wall, mean pore size and the most probable pore size with Barrett-Joyner-Halenda(BJH) diameter are listed in Table 2. As we can see from Table 2, BET surface areas at different molar ratios of CTAB to CTAC were between 740 and 780 m^2/g; the mean pore size with BJH diameter was 3.0 nm or so; the most probable pore size with BJH diameter was

Table 2 BET surface area, pore volume, mean pore size, most probable pore size with BJH diameter and thickness of pore wall at different molar ratios of CTAB to CTAC

Molar ratio of CTAB to CTAC	BET surface area (m^2/g)	Most probable pore size with BJH diameter (nm)	Mean pore size with BJH diameter[a] (nm)	Thickness of pore wall[b](nm)	Total pore volume above 2 nm diameter (cm^3/g)
10:0	769.1	4.10	3.10	1.47	1.56
9:1	739.1	3.95	3.22	1.37	1.40
8:2	786.8	3.33	2.86	1.69	1.28
6.5:3.5	754.9	2.89	3.06	1.47	1.29
5.5:4.5	746.8	4.02	3.01	1.54	1.20

[a] Values calculated from the adsorption portion of N_2 adsorption-desorption isotherm
[b] Thickness of pore wall equaled to a_0 minus mean pore size with BJH diameter

about 2.8~4.0 nm, and thickness of pore wall was 1.47 nm or so. The total pore volumes of mesoporous silica with diameter above 2 nm decreased with decreasing molar ratio of CTAB to CTAC; we thought that electric charge density of micelles was responsible for the above phenomenon. With the decrease of the molar ratio of CTAB to CTAC, the electrostatic interaction between micelles and sodium silicate increased, and the stronger the electrostatic interaction, the more unfavorable the formation of mesoporous silica templated by the mixed micelles of CTAB and CTAC.

To conclude, using sodium silicate as precursors and mixed micelles of CTAB and CTAC as templates, rod-like mesoporous silica was synthesized. With decreasing molar ratio of CTAB to CTAC, the amounts and lengths of rod-like mesoporous silica particles decreased. The resulting mesoporous silica had hexagonal symmetry demonstrated by small-angle XRD. N_2 gas adsorption-desorption curves showed that there existed type IV adsorption isotherm and an H1 hysteresis loop; BET surface area was about 760 m^2/g, mean pore size with BJH diameter was 3.0 nm or so, and thickness of pore wall was about 1.47 nm. Total pore volumes of mesoporous silica of diameter above 2 nm decreased with decreasing molar ratio of CTAB to CTAC.

Acknowledgements This research is supported by State Key Laboratory of New Ceramic and Fine Processes of Tsinghua University and Visiting Scholar Foundation of Key Lab in University.

References

1. Ying JY, Mehnert CP, Wong MS (1999) Angew Chem Int Edn 38:56
2. Huo Q, Margolese DI, Ciesla U, Feng P, Gier TE, Sieger P, Leon R, Petroff PM, Schuth F, Stuky GD (1994) Nature 368:317
3. Lin HP, Mou CY (1996) Science 273:765
4. Lin H-P, Cheng S, Mou C-Y (1998) Chem Mater 10:581
5. Schacht S, Huo Q, Voigt-Martin IG, Stucky GD, Schuth F (1996) Science 273:768
6. Yang H, Coombs N, Ozin GA (1997) Nature 386:692
7. Zhao D, Sun J, Li Q, Stucky GD (2000) Chem Mater 12:275
8. Delsannti M, Moussaid A, Munch JP (1993) J Colloid Interface Sci 157:285
9. Sepúlveda L, Cortés J (1985) J Phys Chem 89:5322
10. Fabre H, Kamunka N, Khan A, Lindblom G, Lindman B (1980) J Phys Chem 84:3428
11. Fengcheng C, Luan Z, Klinowski J (1995) Langmuir 11:2815
12. Sing KSW, Everett DH, Haul RAW, Moscou L, Pierotti RA, Rouquérol J, Siemieniewska T (1985) Pure Appl Chem 57:603